Multi-task Joint Prediction of Infant Cortical Morphological and Cognitive Development

Xinrui Yuan[1,2], Jiale Cheng[2], Fenqiang Zhao[2], Zhengwang Wu[2], Li Wang[2], Weili Lin[2], Yu Zhang[1], and Gang Li[2(✉)]

[1] School of Biomedical Engineering, Southern Medical University, Guangzhou, Guangdong, China

[2] Department of Radiology and Biomedical Research Imaging Center, University of North Carolina at Chapel Hill, Chapel Hill, NC, USA

gang_li@med.unc.edu

Abstract. During the early postnatal period, the human brain undergoes rapid and dynamic development. Over the past decades, there has been increased attention in studying the cognitive and cortical development of infants. However, accurate prediction of the infant cognitive and cortical development at an individual-level is a significant challenge, due to the huge complexities in highly irregular and incomplete longitudinal data that is commonly seen in current studies. Besides, joint prediction of cognitive scores and cortical morphology is barely investigated, despite some studies revealing the tight relationship between cognitive ability and cortical morphology and suggesting their potential mutual benefits. To tackle this challenge, we develop a flexible multi-task framework for joint prediction of cognitive scores and cortical morphological maps, namely, disentangled intensive triplet spherical adversarial autoencoder (DITSAA). First, we extract the mixed representative latent vector through a triplet spherical ResNet and further disentangles latent vector into identity-related and age-related features with an attention-based module. The identity recognition and age estimation tasks are introduced as supervision for a reliable disentanglement of the two components. Then we formulate the individualized cortical profile at a specific age by combining disentangled identity-related information and corresponding age-related information. Finally, an adversarial learning strategy is integrated to achieve a vivid and realistic prediction of cortical morphology, while a cognitive module is employed to predict cognitive scores. Extensive experiments are conducted on a public dataset, and the results affirm our method's ability to predict cognitive scores and cortical morphology jointly and flexibly using incomplete longitudinal data.

Keywords: Cognitive Prediction · Cortical Morphology Prediction · Disentanglement

1 Introduction

The human brain undergoes rapid and dynamic development during the early postnatal period. Research on infant brain development [1–3] has received significant attention over the last decade. While many infant neuroimaging studies have revealed the brain

H. Greenspan et al. (Eds.): MICCAI 2023, LNCS 14228, pp. 545–554, 2023.
https://doi.org/10.1007/978-3-031-43996-4_52

growth patterns during infancy [4–6] at the population level, knowledge on individualized brain development during infancy is still lacking, which is essential for mapping individual brain characteristics to individual phenotypes [7, 8]. Various pioneering methods have been developed using longitudinal scans collected at some pre-defined discrete age time points, such as 3, 6, 9, and 12 months [9–11], which strictly requires each infant has all longitudinal scans at the given time points. However, in practice, longitudinal infant images are usually collected at diverse and irregular scan ages due to the inevitable missing data and imaging protocol design, leading to less usable data. As a result, predicting infant development at specific ages from irregular longitudinal data is extremely challenging, yet critical to understanding normal brain development and early diagnosis of neurodevelopmental abnormalities [12–14]. Besides, to the best of our knowledge, joint prediction of cognitive scores and cortical morphology is barely investigated, despite some studies revealing the tight relationship [15–17] between cognitive ability and cortical morphology, suggesting their potential mutual benefits.

To address this issue, we propose a flexible multi-task framework to jointly predict cognitive score and cortical morphological development of infant brains at arbitrary time points with longitudinal data scanned irregularly within 24 months of age. Specifically, the cognitive ability of each infant was estimated using the Mullen Scales of Early Learning (MSEL) [18], including the visual reception scale (VRS), fine motor scale (FMS), receptive language scale (RLS), and expressive language scale (ELS). Our aim is to predict the four cognitive scores and cortical morphological feature maps (e.g., cortical thickness map) flexibly at arbitrary time points given cortical feature maps at a known age. The main contributions of this paper can be summarized as follows: 1) we propose an attention-based feature disentanglement module to separate the identity- and age-related features from the mixed latent features, which not only effectively extracts the discriminative information at individual-level, but also forms the basis for dealing with irregular and incomplete longitudinal data; 2) we introduce a novel identity conditional block to fuse identity-related information with designated age-related information, which can model the regression/progression process of brain development flexibly; 3) we propose a unified, multi-task framework to jointly predict the cognitive ability and cortical morphological development and enable flexible prediction at any time points during infancy by concatenating the subject-specific identity information and identity conditional block. We validated our proposed method on the Baby Connectome Project (BCP) [19] dataset, including 416 longitudinal scans from 188 subjects, and achieved superior performance on both cognitive score prediction and cortical morphological development prediction than state-of-the-art methods.

2 Methods

2.1 Network Architecture

The framework of our disentangled intensive triplet spherical adversarial autoencoder (DITSAA) is shown in Fig. 1. Since primary and secondary cortical folds in human brains are well established at term birth and keep relatively stable over time, the identity-related cortical features should be approximately time-invariant and age-related features change over time due to brain development. Based on this prior knowledge, we first

disentangle the mixed cortical surface feature maps into age-related and identity-related components. Specifically, in the training stage, we formulate the training samples in triplet units ($S_i^{t_a}, S_i^{t_p}, S_j^{t_n}$), where the first two are surface property maps from the same individual i but at different ages t_a and t_p, and the last one is a surface property map from another individual j at any age t_n. Then we employ the intensive triplet loss [20] to encourage the disentanglement of identity-related features, and age prediction loss to encourage the disentanglement of age-related features.

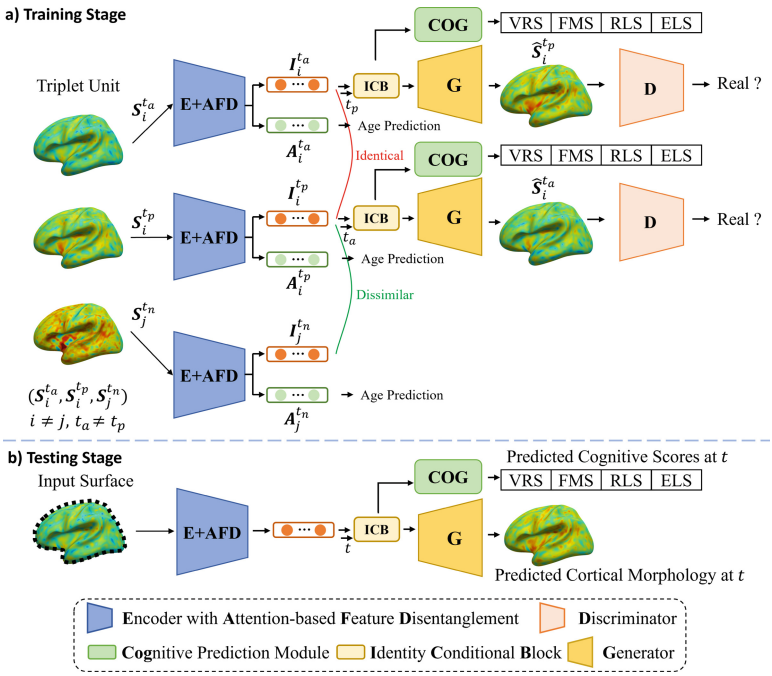

Fig. 1. The framework of the proposed disentangled intensive triplet spherical adversarial autoencoder (DITSAA).

Encoder with Attention-Based Disentanglement. We employ a spherical ResNet, modified based on ResNet [21] and Spherical U-Net [22, 23], denoted as E, as the basic encoder (Fig. 2(a)). The output of the encoder includes multi-level features with different resolutions, and the latent vector z_i^t captures the mixed features of the input cortical surface S_i^t. Then we employ the attention-based feature disentanglement (*AFD*) module, consisting of a channel attention module and a spatial attention module in parallel, to disentangle the age-related variance A_i^t and the identity-related invariance I_i^t, which is defined as: $z_i^t = \underbrace{z_i^t \odot \phi(z_i^t)}_{A_i^t} + \underbrace{z_i^t \odot (1 - \phi(z_i^t))}_{I_i^t}$. The operation $\odot$ indicates the element-wise multiplication and ϕ denotes an attention module in Fig. 2, which is computed as the average of channel attention [24] and spatial attention [25].

Identity Conditional Block. To preserve the identity-level regression/progression pattern, we extended the identity conditional block (*ICB*) [26] to cortical surface data based on spherical convolution. Specifically, the *ICB* takes the identity-related feature from *AFD* as input to learn an identity-level regression/progression pattern. Then, a weight-sharing strategy is adopted to improve the age smoothness by sharing same spherical convolutional filters across adjacent age groups as shown in Fig. 2(b). The idea of the weight-sharing strategy is that age-related features change gradually over time, and the shared filters can learn common evolving patterns between adjacent age groups. Then, we can select the features of the target age, which we call the identity-level age condition as shown in Fig. 2(b). Note that the percentage of shared features is empirically set to 0.1 and the filter number of each age group is set to 64. Therefore, the feature number of the regression/progression pattern is: $\lfloor (age_{group} - (age_{group} - 1) \times 0.1) \times 64 \rfloor = 1,388$, where age_{group} is 24, denoting 24 months of age.

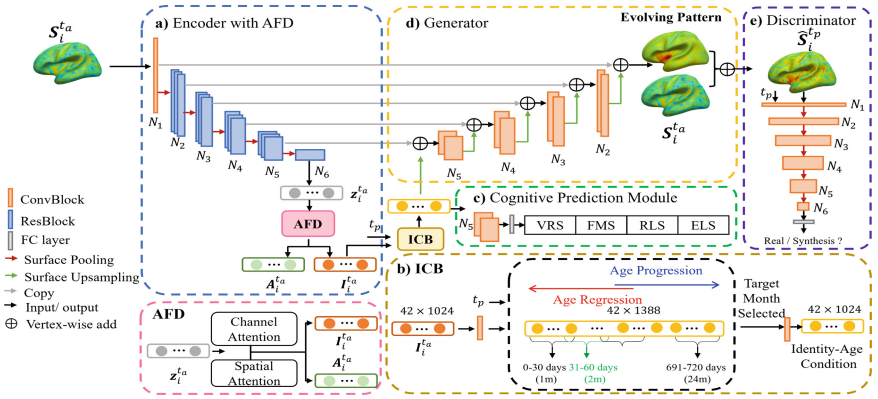

Fig. 2. Illustration of a branch of DITSAA, which consists of five major components: a) the encoder E with attention-based feature disentanglement module (*AFD*), b) the identity conditional block (*ICB*), c) the cognitive prediction module (*COG*) for cognitive prediction, d) the generator G, and e) the discriminator D for cortical morphological map. Each residual block (ResBlock) contains repeated 1-ringConv + BN + ReLU with reslink. Each convolutional block (ConvBlock) contains 1-ringConv + BN + ReLU. Of note, the ConvBlock in generator contains additional spherical transposed convolution layer to deal with the concatenation of multi-level features. N_k denotes the number of vertices in the spherical feature maps at the k-th icosahedron subdivision, where $N_{k+1} = (N_k + 6)/4$, while in our experiments N_1 equals to 40,962. The number of features after each operation block is [64, 128, 256, 512, 1024, 1024] for the k-th icosahedron subdivision ($k \in [1, 6]$).

Cognition Prediction Module. To accurately predict individual-level cognitive scores, we use the identity-age condition features containing subject-specific information and conditional age features to predict the cognitive scores through a spherical convolutional network *COG* (Fig. 2(c)). The predicted cognitive scores are computed as: $\hat{\boldsymbol{y}}_i^{t_p} = COG\left(\boldsymbol{S}_i^{t_a}, t_p\right) = COG\left(ICB\left(\boldsymbol{I}_i^{t_a}, t_p\right)\right)$.

Cortical Morphology Prediction Module. To ensure the quality of the predicted cortical morphological maps, the generator G adopts the architecture of the UNet-based least-square GANs [27]. For the discriminator D, we extend a VGG style classification CNN to spherical surfaces. The generator G takes the selected identity-age conditional features $ICB\left(\boldsymbol{I}_i^{t_a}, t_p\right)$ as inputs and gradually upsamples them and concatenates with the corresponding-level features produced by the encoder as shown in Fig. 2, and aims to predict the target cortical surface map $\hat{\boldsymbol{S}}_i^{t_p}$. This process can be summarized as: $\hat{\boldsymbol{S}}_i^{t_p} = G\left(\boldsymbol{S}_i^{t_a}, t_p\right) = G\left(\left[E\left(\boldsymbol{S}_i^{t_a}\right); ICB\left(\boldsymbol{I}_i^{t_a}, t_p\right)\right]\right)$, $[\cdot;\cdot]$ denotes the concatenation along the channel dimension.

2.2 Loss Design

Intensive Triplet Loss. As illustrated in Fig. 1, we suppose identity-related invariance $\boldsymbol{I}$ from a pair of same subjects $(\boldsymbol{S}_i^{t_a}, \boldsymbol{S}_i^{t_p})$ should be identical, while that from a pair of different subjects $(\boldsymbol{S}_i^{t_a}, \boldsymbol{S}_j^{t_n})$ should be dissimilar. However, noticing that $(\boldsymbol{S}_i^{t_p}, \boldsymbol{S}_j^{t_n})$ is also a pair of different subjects, to enhance the relative distance between same subject pair and all the different subject pairs, we apply the intensive triplet loss [20] to help AFD extract identity-related features thoroughly from latent features. A simple linear network denoted as ID is designed to extract feature vector of identity-related feature $\boldsymbol{I}$ and the feature similarity is measured by Pearson's correlation coefficient ($Corr$):

$$\begin{aligned} L_{IT} = -2 * Corr\left(ID\left(\boldsymbol{I}_i^{t_a}\right), ID\left(\boldsymbol{I}_i^{t_p}\right)\right) \\ + \left(Corr\left(ID\left(\boldsymbol{I}_i^{t_a}\right), ID\left(\boldsymbol{I}_j^{t_n}\right)\right) + Corr\left(ID\left(\boldsymbol{I}_i^{t_p}\right), ID\left(\boldsymbol{I}_j^{t_n}\right)\right)\right) \end{aligned} \tag{1}$$

Age Estimation Loss. To ensure AFD extracts the age-relation information, a simple network is designed as the regressor $AgeP$ to predict age from age-related variance $\boldsymbol{A}$. The regressor $AgeP$ has three fully connected layers with 512, 720, and 24 neurons, respectively. It aims to predict the age by computing a softmax expected value [28]:

$$L_{AE} = \left\|AgeP\left(\boldsymbol{A}_i^{t_a}\right) - t_a\right\|_1 + \left\|AgeP\left(\boldsymbol{A}_i^{t_p}\right) - t_p\right\|_1 + \left\|AgeP\left(\boldsymbol{A}_j^{t_n}\right) - t_n\right\|_1. \tag{2}$$

Cognitive Prediction Loss. Given the identity-related age condition derived from ICB, we regress the cognitive scores directly by the cognitive prediction module at a selected age t. The loss function to train the cognitive prediction module is defined as:

$$L_{Cog} = \|\boldsymbol{y}_i^{t_a} - \hat{\boldsymbol{y}}_i^{t_a}\|_1 + \|\boldsymbol{y}_i^{t_p} - \hat{\boldsymbol{y}}_i^{t_p}\|_1, \tag{3}$$

where $\boldsymbol{y}$ is the ground truth of cognitive scores.

Adversarial Loss. To improve the quality of the predicted cortical property maps, we used the adversarial loss to train the generator G and discriminator D with respect to least-square GANs [27]. The aim of the discriminator D is to distinguish the generated cortical property maps as fake data, while the original cortical property maps as real

data. The generator G aims to generate cortical property maps as close to the real data as possible. Thus, the objective function is expressed as:

$$\min_D L_D = 0.5\Big[D\Big(\Big[S_i^{t_a}; C_{t_a}\Big]\Big) - 1\Big]^2 + 0.5\Big[D\Big(\Big[\widehat{S}_i^{t_p}; C_{t_p}\Big]\Big)\Big]^2, \tag{4}$$

$$\min_G L_G = 0.5\Big[D\Big(\Big[\widehat{S}_i^{t_p}; C_{t_p}\Big]\Big) - 1\Big]^2, \tag{5}$$

where C_t denotes the one-hot age encoding at different age t.

Reconstruction Loss. To guarantee the high-quality reconstruction and constrain the vertex-wise similarity of the input cortical morphological features and generated cortical morphological features, we adopted the L1 loss to evaluate the reconstruction:

$$L_{rec} = \|\widehat{S}_i^{t_a} - S_i^{t_a}\|_1 + \|\widehat{S}_i^{t_p} - S_i^{t_p}\|_1. \tag{6}$$

Full Objective. The objective functions of our model are written as:

$$L_{(E,ID,AgeP)} = \lambda_{IT} L_{IT} + \lambda_{AE} L_{AE}, \tag{7}$$

$$L_{(ICB,Cog,G,D)} = \lambda_{Cog} L_{Cog} + \lambda_D L_D + \lambda_G L_G + \lambda_{rec} L_{rec}, \tag{8}$$

where λ_{IT}, λ_{AE}, λ_{Cog}, λ_G, λ_D, and λ_{rec} control the relative importance of the loss terms.

3 Experiments

3.1 Dataset and Experimental Settings

In our experiments, we used the public BCP dataset [19] with 416 scans from 188 subjects (104 females/84 males) within 24 months of age, where 71 subjects have the single-time-point scans, and 117 subjects have multi-time-point scans. Cortical surface maps were generated using an infant-dedicated pipeline (http://www.ibeat.cloud/) [5]. All cortical surface maps were mapped onto the sphere [29] and registered onto the age-specific surface atlases (https://www.nitrc.org/projects/infantsurfatlas/) [6, 30] and further resampled to have 40,962 vertices. We chose 70% of subjects with multi-time-point scans as the train-validation set and conducted a 5-fold cross-validation for tuning the best parameter setting and left 30% for the test set. Of note, subjects with single-time-point scans were unable to evaluate the performance of prediction, hence, they were solely included in the training set to provide additional developmental information.

We trained E, ID, and $AgeP$ using an SGD optimizer under the supervision of L_{AE} and L_{IT} with an initial learning rate of 0.1, momentum of 0.9, and a self-adaption strategy for updating the learning rate, which was reduced by a factor of 0.2 once the training loss stopped decreasing for 5 epochs, and the hyper-parameters in the training loss functions were empirically set as follows: λ_{AE} was 0.1 and λ_{IT} was 0.1. We then fixed E and used an Adam optimizer with an initial learning rate of 0.01, β_1 of 0.5, and β_2 of 0.999 to train ICB, COG, G, and D using Eq. (8) with a self-adaption strategy for updating the

learning rate. The hyper-parameters in the loss functions are empirically set as follows: $\lambda_D = 1$, $\lambda_G = 35$, $\lambda_{Cog} = 0.1$, and $\lambda_{rec} = 0.1$.

We used the cortical thickness map at one time point to jointly estimate the four Mullen cognitive scores, i.e., VRS, FMS, RLS, and ELS, and the cortical thickness map at any other time points. To quantitatively evaluate the cognitive prediction performance, the Pearson's correlation coefficient (PCC) between the ground truth and predicted values was calculated. For the cortical morphology prediction, the PCC and mean absolute error (MAE) between the ground truth and predicted values were calculated. In the testing phase, the mean and standard deviation of the 5-fold results were reported.

3.2 Evaluation and Comparison

To comprehensively evaluate the mutual benefits of the proposed modules in cognitive and cortical morphological development prediction, we conducted an ablation study on two modules in Table 1, where *w/Cognitive* and *w/Cortical* respectively denotes the variant for training cognitive prediction module and cortical prediction module only, and *w/o AFD* denotes the variant for training whole framework without *AFD* module. It can be observed that, the performance on cognitive and cortical prediction tasks has been improved by performing two tasks jointly, which highlights the associations and mutual benefits between cortical morphology and cognitive ability during infant brain development.

Table 1. Performance of different variants on both cognitive (first four columns) and cortical morphological property prediction (last column). * indicates statistically significantly better results than other methods with p-value < 0.05.

Variants	ELS	FMS	RLS	VRS	MAE
w/Cognitive	0.745 ± 0.022	0.868 ± 0.005	0.806 ± 0.024	0.769 ± 0.014	/
w/Cortical	/	/	/	/	0.507 ± 0.057
w/o AFD	0.774 ± 0.040	$\mathbf{0.888 \pm 0.026}$	0.828 ± 0.039	0.790 ± 0.034	0.322 ± 0.044
Proposed	$\mathbf{0.806 \pm 0.016}$*	0.880 ± 0.012	$\mathbf{0.850 \pm 0.004}$*	$\mathbf{0.820 \pm 0.014}$*	$\mathbf{0.312 \pm 0.032}$*

We also compared our DITSAA with various existing methods given different tasks in our multi-task framework. For the cortical morphology and cognitive development prediction, the state-of-the-art spherical networks SUNet [22], UGSCNN [31], and Spherical Transformer [32] were utilized as baselines. However, these networks are unable to flexibly predict cortical morphology at any time point. Therefore, we apply one-hot encoding to specify the age condition and concatenate it with the cortical morphological features along the channel attention as input to predict cognitive scores and cortical thickness at specific time point. Note that these methods with one-hot age condition still lack the generality and exhibit unsatisfactory performance in predicting both cognition and cortical morphological properties with only a few training samples at each month due to the irregularity of the longitudinal dataset [19]. As illustrated in Table 2 and Fig. 3, we can see our proposed DITSAA achieves better performance in both cortical morphological and cognitive development prediction.

Table 2. Comparison with other state-of-the-art methods on both cognitive (first four columns) and cortical morphological property prediction (last two columns) tasks. * indicates statistically significantly better results than other methods with p-value < 0.05.

Methods	ELS	FMS	RLS	VRS	MAE	PCC
SUNet	0.377 ± 0.033	0.339 ± 0.427	0.368 ± 0.055	0.304 ± 0.042	0.524 ± 0.141	0.872 ± 0.182
UGSCNN	0.223 ± 0.117	0.154 ± 0.025	0.185 ± 0.021	0.193 ± 0.089	0.548 ± 0.065	0.849 ± 0.164
Spherical Transformer	0.186 ± 0.045	0.118 ± 0.058	0.198 ± 0.052	0.181 ± 0.035	0.575 ± 0.123	0.861 ± 0.121
Proposed	$\mathbf{0.806 \pm 0.016}^*$	$\mathbf{0.880 \pm 0.012}^*$	$\mathbf{0.850 \pm 0.004}^*$	$\mathbf{0.820 \pm 0.014}^*$	$\mathbf{0.312 \pm 0.032}^*$	$\mathbf{0.893 \pm 0.103}^*$

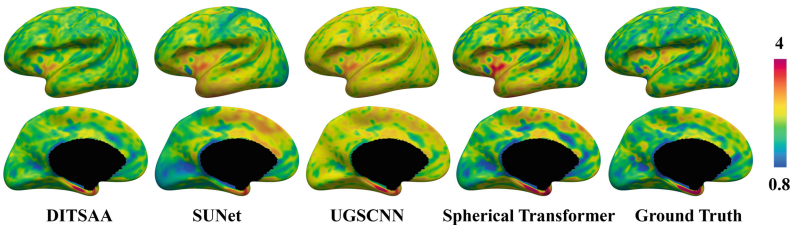

Fig. 3. The predicted cortical morphology property maps (herein, cortical thickness (mm)) of a randomly selected subject (predicted from 4 to 7 months of age) obtained by proposed DITSAA and other competing methods.

4 Conclusions

In this study, we proposed a novel flexible multi-task joint prediction framework for infant cortical morphological and cognitive development, named disentangled intensive triplet spherical adversarial autoencoder. We effectively and sufficiently leveraged all existing longitudinal infant scans with highly irregular and nonuniform age distribution. Moreover, we leverage the mutual benefits between cortical morphological and cognitive development to improve the performance of both tasks. Our framework enables jointly predicting cortical morphological and cognitive development flexibly at arbitrary ages during infancy, both regression and progression. The promising results on the BCP dataset demonstrate the potential power for individual-level development prediction and modeling.

Acknowledgements. This work was supported in part by NIH grants (MH116225, MH117943, MH127544, and MH123202). This work also utilizes approaches developed by an NIH grant (1U01MH110274) and the efforts of the UNC/UMN Baby Connectome Project Consortium.

References

1. Casey, B., Tottenham, N., Liston, C., Durston, S.: Imaging the developing brain: what have we learned about cognitive development? Trends Cogn. Sci. **9**(3), 104–110 (2005)

2. Dubois, J., Hertz-Pannier, L., Cachia, A., Mangin, J.F., Le Bihan, D., Dehaene-Lambertz, G.: Structural asymmetries in the infant language and sensorimotor networks. Cereb. Cortex **19**(2), 414–423 (2009)
3. Smyser, C.D., Inder, T.E., Shimony, J.S., Hill, J.E., Degnan, A.J., Snyder, A.Z., et al.: Longitudinal analysis of neural network development in preterm infants. Cereb. Cortex **20**(12), 2852–2862 (2010)
4. Gilmore, J.H., Kang, C., Evans, D.D., Wolfe, H.M., Smith, J.K., Lieberman, J.A., et al.: Prenatal and neonatal brain structure and white matter maturation in children at high risk for schizophrenia. Am. J. Psychiatry **167**(9), 1083–1091 (2010)
5. Wang, L., Wu, Z., Chen, L., Sun, Y., Lin, W., Li, G.: iBEAT v2. 0: a multisite-applicable, deep learning-based pipeline for infant cerebral cortical surface reconstruction. Nat. Protocols **18**, 1488–1509 (2023)
6. Li, G., Wang, L., Shi, F., Gilmore, J.H., Lin, W., Shen, D.: Construction of 4D high-definition cortical surface atlases of infants: Methods and applications. Med. Image Anal. **25**(1), 22–36 (2015)
7. Kanai, R., Rees, G.: The structural basis of inter-individual differences in human behaviour and cognition. Nat. Rev. Neurosci. **12**(4), 231–242 (2011)
8. Mueller, S., Wang, D., Fox, M.D., Yeo, B.T., Sepulcre, J., Sabuncu, M.R., et al.: Individual variability in functional connectivity architecture of the human brain. Neuron **77**(3), 586–595 (2013)
9. Fishbaugh, J., Prastawa, M., Gerig, G., Durrleman, S.: Geodesic regression of image and shape data for improved modeling of 4D trajectories. In: 2014 IEEE 11th International Symposium on Biomedical Imaging (ISBI), pp. 385–388. IEEE (2014)
10. Rekik, I., Li, G., Lin, W., Shen, D.: Predicting infant cortical surface development using a 4D varifold-based learning framework and local topography-based shape morphing. Med. Image Anal. **28**, 1–12 (2016)
11. Meng, Y., Li, G., Rekik, I., Zhang, H., Gao, Y., Lin, W., et al.: Can we predict subject-specific dynamic cortical thickness maps during infancy from birth? Hum. Brain Mapp. **38**(6), 2865–2874 (2017)
12. Lin, W., Zhu, Q., Gao, W., Chen, Y., Toh, C.H., Styner, M., et al.: Functional connectivity mr imaging reveals cortical functional connectivity in the developing brain. Am. J. Neuroradiol. **29**(10), 1883–1889 (2008)
13. Ecker, C., Shahidiani, A., Feng, Y., Daly, E., Murphy, C., D'Almeida, V., et al.: The effect of age, diagnosis, and their interaction on vertex-based measures of cortical thickness and surface area in autism spectrum disorder. J. Neural Transm. **121**, 1157–1170 (2014)
14. Querbes, O., et al.: Early diagnosis of alzheimer's disease using cortical thickness: impact of cognitive reserve. Brain **132**(8), 2036–2047 (2009)
15. Girault, J.B., Cornea, E., Goldman, B.D., Jha, S.C., Murphy, V.A., Li, G., et al.: Cortical structure and cognition in infants and toddlers. Cereb. Cortex **30**(2), 786–800 (2020)
16. Kagan, J., Herschkowitz, N.: A Young Mind in a Growing Brain. Psychology Press (2006)
17. Cheng, J., Zhang, X., Ni, H., Li, C., Xu, X., Wu, Z., et al.: Path signature neural network of cortical features for prediction of infant cognitive scores. IEEE Trans. Med. Imaging **41**(7), 1665–1676 (2022)
18. Mullen, E.M., et al.: Mullen Scales of Early Learning. AGS Circle Pines, MN (1995)
19. Howell, B.R., Styner, M.A., Gao, W., Yap, P.T., Wang, L., Baluyot, K., et al.: The UNC/UMN baby connectome project (BCP): an overview of the study design and protocol development. Neuroimage **185**, 891–905 (2019)
20. Hu, D., et al.: Disentangled intensive triplet autoencoder for infant functional connectome fingerprinting. In: Martel, A.L., et al. (eds.) MICCAI 2020. LNCS, vol. 12267, pp. 72–82. Springer, Cham (2020). https://doi.org/10.1007/978-3-030-59728-3_8

21. He, K., Zhang, X., Ren, S., Sun, J.: Deep residual learning for image recognition. In: Proceedings of the IEEE Conference on Computer Vision and Pattern Recognition. pp. 770–778 (2016)
22. Zhao, F., Wu, Z., Wang, L., Lin, W., Gilmore, J.H., Xia, S., et al.: Spherical deformable U-net: application to cortical surface parcellation and development prediction. IEEE Trans. Med. Imaging **40**(4), 1217–1228 (2021)
23. Zhao, F., Xia, S., Wu, Z., Duan, D., Wang, L., Lin, W., et al.: Spherical U-net on cortical surfaces: methods and applications. In: Chung, A., Gee, J., Yushkevich, P., Bao, S. (eds.) IPMI 2019. LNCS, vol. 11492, pp. 855–866. Springer, Cham (2019). https://doi.org/10.1007/978-3-030-20351-1_67
24. Hu, J., Shen, L., Sun, G.: Squeeze-and-excitation networks. In: Proceedings of the IEEE Conference on Computer Vision and Pattern Recognition,pp. 7132–7141 (2018)
25. Woo, S., Park, J., Lee, J.Y., Kweon, I.S.: CBAM: convolutional block attention module. In: Proceedings of the European Conference on Computer Vision (ECCV). pp. 3–19 (2018)
26. Huang, Z., Zhang, J., Shan, H.: When age-invariant face recognition meets face age synthesis: a multi-task learning framework and a new benchmark. IEEE Trans. Pattern Anal. Mach. Intell. **45**(6), 7917–7932 (2023)
27. Mao, X., Li, Q., Xie, H., Lau, R.Y., Wang, Z., Paul Smolley, S.: Least squares generative adversarial networks. In: Proceedings of the IEEE International Conference on Computer Vision, pp. 2794–2802 (2017)
28. Rothe, R., Timofte, R., Van Gool, L.: DEX: deep expectation of apparent age from a single image. In: Proceedings of the IEEE International Conference on Computer Vision Workshops, pp. 10–15 (2015)
29. Fischl, B.: Freesurfer. NeuroImage **62**(2), 774–781 (2012)
30. Wu, Z., Wang, L., Lin, W., Gilmore, J.H., Li, G., Shen, D.: Construction of 4D infant cortical surface atlases with sharp folding patterns via spherical patch-based group-wise sparse representation. Hum. Brain Mapp. **40**(13), 3860–3880 (2019)
31. Jiang, C.M., Huang, J., Kashinath, K., Prabhat, Marcus, P., Nießner, M.: Spherical CNNs on unstructured grids. In: ICLR (Poster) (2019)
32. Cheng, J., et al.: Spherical transformer on cortical surfaces. In: Lian, C., Cao, X., Rekik, I., Xu, X., Cui, Z. (eds.) MLMI 2022. LNCS, vol. 13583, pp. 406–415. Springer, Cham (2022). https://doi.org/10.1007/978-3-031-21014-3_42